Next Materials 7 (2025) 100384

Contents lists available at ScienceDirect

Next Materials

journal homepage: www.sciencedirect.com/journal/next-materials

Research article

Enhancing Venetian traditional marmorino with TiO_2 and ZnO for antimicrobial protection – A case study

Andrea Campostrini [a], Sabrina Manente [a], Elena Ghedini [a], Alessandro Di Michele [b], Federica Menegazzo [a,*]

[a] Department of Molecular Sciences and Nanosystems, Ca' Foscari University of Venice, Via Torino 155, Venice 30170, Italy
[b] Department of Physics and Geology, University of Perugia, Via A. Pascoli, Perugia 06123, Italy

ARTICLE INFO

Keywords:
Marmorino plasters
Photocatalysts
TiO_2
ZnO
Biocidal properties
Venetian palaces

ABSTRACT

Venetian marmorino is a traditional plaster that has been used since the 15th century, in several palaces in Venice and ancient villas throughout the Veneto region. While this material has considerable durability, it remains susceptible to various surface degradation processes. An effective means to mitigate such events is through the application of photocatalytic coatings. These coatings employ just oxygen from the atmosphere and light as energy source to degrade both organic and inorganic environmental pollutants, confer self-cleaning properties, and reduce bacterial attacks or fungal growth.

In this work titania (TiO_2) and zinc oxide (ZnO) were incorporated into the marmorino, both as top coating and within the mortar itself. The biocidal efficacy of these additives was assessed through optical microscopic observations of fungal colonies grown on the marmorino mock-ups with differing compositions or finish layers. Two Fungi *Penicillium italicum and Cladosporium spherospermum* were selected as reference microorganisms attacking wall materials in Venice. Hence, a more detailed analysis utilizing electron microscopy (SEM) was conducted to confirm the biocidal properties.

The experimental results demonstrate that the development of a high-tech multifunctional marmorino capable not only of reducing environmental pollutants but of preventing surface degradation and inhibiting fungal growth. This inhibition leads to a reduction in biodegradation, resulting in a diminished ability to take root and lack of spore development.

1. Introduction

Venetian *marmorino* is a traditional plaster widely employed as wall coating in several ancient buildings in Venice and in the Veneto region [1–5]. *Marmorino* has been employed both as plaster for new constructions and as material for restoration interventions of ancient ones [6–8].

The stratigraphy of *marmorino* typically comprises multiple thin layers of sand-based plaster applied in a *fresco su fresco* technique without waiting for the lime putty ($Ca(OH)_2$) to fully carbonate. Notably, the final mortar layer incorporates fine-grained marble powder ($CaCO_3$) alongside lime putty [9]. Traditionally, several natural substances such as soap, lime water, or natural oils were applied as finish layer, either before the carbonation process or afterward, to provide both protection and desired optical properties [10,11].

Despite its intrinsic protective features, *marmorino* surfaces exposed to modern pollutants face greater environmental challenges [12–21]. Volatile Organic Compound (VOC) pollutants, often deposited as thin layers not only contribute to chemical and physical degradation but also facilitate biodegradation processes [22,23]. Biodegradation includes all the undesirable changes in mater properties accelerated by microbial activity across various taxonomic groups [24,25].

The combination of environmental factors (*i.e.*, moisture, light, temperature, surface deposits, ventilation, capillary rise, and pollutants) eases the deterioration of the walls and the increase of the surface porosity [26–28]. This makes the surface more bio-receptive, encouraging the ecological flow growth of bacterial and fungal consortia, plant-like organisms, and even herbal to arbustive plants [29–31]. This heightened susceptibility to biodeterioration can foster the establishment of an ecosystem on stone surfaces. Biodeteriogens act on surfaces through different, but all dangerous, mechanisms [32–35].

While several approaches exist to remove such deposits and restore the surface, they often involve products applied after damage has

* Corresponding author.
E-mail address: federica.menegazzo@unive.it (F. Menegazzo).

https://doi.org/10.1016/j.nxmate.2024.100384
Received 16 September 2024; Accepted 23 September 2024
Available online 30 September 2024

occurred [36–38]. An appealing alternative is the use of materials capable of preventing deposit formation or chemically removing them as they begin to form [39]. Photocatalytic materials are well-suited for this purpose, as they can trigger beneficial chemical reactions employing atmospheric oxygen and sunlight energy. Photocatalysts can induce reactions that interact with common air pollutants, degrade surface degradation compounds, and even mitigate the growth of biological organisms that deposit, adhere, and proliferate on the wall surface [40].

Titanium dioxide (TiO_2) is the most employed photocatalytic material in various applications [41–43]. Consequently, it is also being investigated as component in photoactive wall coatings, either for its biocidal effect to inhibit biodeterioration or for its self-bleaching effect to prevent the formation of stains due to pollution or vandalism [44,45]. Zinc oxide (ZnO) is another semiconductor employed for its self-bleaching properties. Moreover, it is well-known for its potent biocidal properties in various applications [46,47]. As previously demonstrated by the authors [48], appropriate TiO_2 and ZnO photocatalysts do not cause color variation when applied to *marmorino* surfaces, thereby preserving the aesthetic integrity of the stone – an essential characteristic when dealing with Cultural Heritage materials [44]. Furthermore, they both demonstrated great self-cleaning surface characteristics, capable of degrading model stain compounds [48,49], such as methylene blue or methylene red, as well as real-case stain compounds like blue pen, various markers, or food residues [50]. Previous results also demonstrated that the combination of photocatalytic materials with Aleppo's natural soap in the finish layer exhibited even higher efficacy [48]. This last aspect could also avoid the detachment of the photocatalysts from the surface, leading to a more stable material.

For these reasons, both TiO_2 and ZnO are employed and investigated for their antimicrobial activity to combat fungal proliferation even on stone surfaces [51–53]. Literature studies suggest that these materials can be applied primarily as a superficial coating on different types of stone surfaces [54–58] or even incorporated into the mortar in the case of concrete or plasters [59,60]. In the former case, the metal-based oxides primarily exploit photocatalytic phenomena, which cannot be fully used when incorporating the photocatalyst as a component of the mortar matrix. Nevertheless, studies report that employing metal oxides (*e.g.,* ZnO, CaO, MgO) within the material formulation, the particles still inhibit dangerous microorganisms' growth [59]. Therefore, the antimicrobic phenomenon cannot exclusively be attributed to the photocatalytic actions of ZnO but rather to failures in the microorganisms' proliferation and reproduction processes induced by the particle composition. The active oxygen species generated by the ZnO particles is considered the primary mechanism of antibacterial activity [61–65].

2. Research aim

In this work, our objective was to modify the formulation of Venetian *marmorino* plaster by incorporating TiO_2 and ZnO, aiming to confer inhibition properties against microorganisms' growth. Titanium-based materials were employed for surface coating, while ZnO was integrated into the *marmorino* plaster formulation. Optical and electron microscopy (SEM) were employed to establish the inhibition action of ZnO and TiO_2 on fungal cultures inoculated on the surface of the *marmorino* mock-ups.

Previous works extensively characterized the photocatalytic plaster mock-ups and studied their activity towards self-cleaning features [48,50], while this study focuses on investigating the impact of added photocatalysts on the antimicrobial properties of these materials. To the best of the authors' knowledge, there are no specific studies regarding this aspect, applied to plaster-like stone materials.

3. Materials and methods

3.1. Materials

To synthetize the photocatalysts the reagents were used as-received: $TiOSO_4 \cdot xH_2O \cdot yH_2SO_4$, $Zn(NO_3)_2 \cdot 6\ H_2O$, titanium (IV) isopropoxide, $Na_2CO_3NH_3$ aqueous solution, and isopropanol were purchased from Sigma Aldrich. The commercial photocatalysts employed were TiO_2 P25 from Evonik (Essen, Germany) and ZnO from CARLO ERBA Reagents S.r.l. (Milan, Italy). For what concerns the *marmorino* mock-ups preparation, the quicklime (CaO) and the marble powders (*impalpabile* and *spolverone* – $CaCO_3$) were provided by Uni.S.Ve. company (Venice, Italy).

For the microbiological growth, maintenance, and testing, the reagents were used as received: Sabouraud Dextrose Agar (SDA), Malt Extract Agar (MEA), and Nutrient Broth (NB) were purchased from Biolife (Milan, Italy), whereas the 5 % saline solution (NaCl) was purchased from Sigma Aldrich.

Finally, for what concerns the SEM measurements samples preparation, Conducting Carbon Cement (Leit-C) was employed.

3.2. Methods

3.2.1. Photocatalysts preparation

The photocatalysts (TiO_2, ZnO, ZnO-TiO_2 composite) were prepared following a procedure previously reported by the authors [48,66,67] and labeled Ti-LAB, Zn-LAB, and TiZn-LAB respectively. Briefly, a 1.2 M aqueous solution of $TiOSO_4$ precursor was added dropwise to 200 mL of H_2O, while maintaining the pH at a constant value of 5.5 using 9 M aqueous NH_3. Afterward, the suspension was aged at 60°C for 20 hours, washed on a Gooch filter, and air-dried at 110°C for 18 hours. The resulting material was hence annealed at 400°C for 4 hours in an airflow of 30 mL/min and then labeled as Ti-LAB.

Similarly, laboratory-made ZnO was prepared using a 1.1 M aqueous solution of $Zn(NO_3)_2{\cdot}6\ H_2O$ and 1.0 M Na_2CO_3 aqueous solution as the precipitating agent, while maintaining a pH of 9 during the precipitation process. This sample was labeled as Zn-LAB.

Finally, a zinc oxide-titanium dioxide composite material, containing a theoretical amount of 10 % wt of TiO_2, was prepared via wetness impregnation. This involved dissolving a proper amount of titanium precursor (Ti(IV) isopropoxide) in isopropanol. The impregnated sample was then air-dried at 110°C for 18 hours and subsequently annealed at 400°C for 4 hours in an airflow of 30 mL/min. In this way a core-shell like structure was obtained. This sample was labeled ZnTi-LAB.

The two benchmark products, used as references, were TiO_2 P25 from Evonik and ZnO from Carlo Erba, and were respectively labeled Ti-COM and Zn-COM.

In Table 1 are briefely reported the results previously obtained by the authors in the photocatalytic materials characterizations:

3.2.2. Marmorino mock-ups preparation

The *marmorino* plaster mock-ups were prepared following the traditional Venetian recipe provided by the Uni.S.Ve. s.r.l. restoration company [50], applying different kinds of finish layers: no finish layer, traditional (Aleppo soap), Aleppo soap + TiO_2.

Table 1
photocatalytic materials characteristics.

Sample	Crystallite size (nm)	Crystalline phase	BET surface area (m^2/g)
Ti-COM	20	anatase, ruthile	52
Ti-LAB	9	anatase	120
Zn-COM	158	wurzite	5
Zn-LAB	15	wurzite	42
ZnTi-LAB	17	wurzite, anatase	33

Briefly, a laboratory-made Venetian *marmorino* was applied to a 20 × 20 cm *cotto* brick. Initially, an underlayer comprising coarse sand and lime putty in a 1:3 wt ratio was applied to a wet brick surface. Afterward, two layers of *marmorino* were applied. These layers consisted of *impalpabile*, a finely powdered marble (0.07 mm), *spolverone*, a coarser marble powder (1–3 mm), and lime putty in a 2:1:1 wt ratio. A third layer of marmorino was then applied, composed by combining 16 g of the aforementioned calcium-based mixture with either 4 g of photocatalyst or 4 g of impalpabile.

For what concerns the finish layers, the traditional Aleppo soap was compared with an innovative one characterized by Aleppo Soap enriched with TiO_2 NPs, namely Evonik P25 (Ti-COM). A comparison with a pristine, not treated sample was also carried out. The preparation of the traditional finish layer, 50 mg of Aleppo soap were diluted with 2.5 mL of H_2O, then placed in an ultrasonic bath for 30 minutes at at T = 50°C. They were subsequently collected and applied with a brush to the dedicated section. For the section reserved for the finish with Aleppo soap and Ti-COM, 50 mg of Alesppo soap were combined with 25 mg of Ti-COM, diluted in 2.5 mL of H_2O, and the same procedure as the previous application was followed.

Finally, the mock-ups were left at RT for 20 days to dry and carbonatate.

Table 2
Mock-ups and samples descriptions.

Last *marmorino* plaster layer	Finish layer	Sample with *Penicillium italicum*	Sample with *Cladosporium spherospermum*
Marble powder + lime putty + *impalpabile* marble powder	No finish layer	A1p	A1c
	Traditional (Aleppo soap)	A2p	A2c
	Aleppo soap + TiO_2	A3p	A3c
Marble powder + lime putty + Zn-COM	No finish layer	B1p	B1c
	Traditional (Aleppo soap)	B2p	B2c
	Aleppo soap + TiO_2	B3p	B3c
Marble powder + lime putty + Zn-LAB	No finish layer	C1p	C1c
	Traditional (Aleppo soap)	C2p	C2c
	Aleppo soap + TiO_2	C3p	C3c
Marble powder + lime putty + ZnTi-LAB	No finish layer	D1p	D1c
	Traditional (Aleppo soap)	D2p	D2c
	Aleppo soap + TiO_2	D3p	D3c

3.2.3. Microorganisms sampling campaign

To select the microorganisms to be used, a sampling campaign was conducted on real-case *marmorino* plasters found on the external walls of some palaces dating back approx. 1500–1700 in Venice (Fig. 1S). The sampling process involved non-invasive methods using *Fungi-Tape*™ adhesive tape (Fisher Scientific) and sterile cotton swabs.

The *Fungi-Tape*™ samplings were examined under the optical microscope, while the cotton swabs were plated on Petri dishes with different cultivation mediums (SDA, MEA, NB, MEA+ NaCl 5 %). The Petri dishes were then incubated at 21.5 ± 2 °C for 7 days to allow initial mycelium development and monitored for up to 20 days for fungal colony growth until maturation (active and abundant sporulation).

At this stage, the identified Fungi, *Penicillium italicum* and *Cladosporium spherospermum*, were selected for the study based on their growth and morphology [68]. These Fungi were isolated and allowed to grow in pure axenic culture using MEA cultivation medium for 5 days in an incubator at 21.5 ± 2 °C, until optimal inoculation growth levels were reached.

3.2.4. Marmorino antimicrobial activity test

Based on literature [47,69], a system was developed to study the antimicrobial properties of the *marmorino* mock-ups. These mock-ups were tested by applying a Fungi inoculum, cut using a microbiology cork borer, onto their surfaces, and observing the resulting fungal growth. The growth test spanned a month period, maintaining a humid environment and a controlled temperature of 23 ± 2°C to ease the Fungi spreading. The mock-ups were kept in a humid environment undergoing to natural nyctemeral cycles, to better reproduce the influence of environmental factors.

During the growth test, fungal growth was evaluated through a photographic campaign of the plaster mock-ups. After the test concluded, more detailed microscope analyses were conducted. Initially, the mock-up surfaces were sampled using *Fungi-Tape*™, which were then affixed onto glass slides for microscopy observation of the fungal growth state. The monitoring of fungal growth involved observations using a stereoscope Stemi SV 6 (ZEISS, Germany) and an optical microscope Axioplan (ZEISS, Germany) at different magnifications. Instantaneous images were acquired using an incorporated digital camera AxioCam ERc5s (ZEISS, Germany) and processed using the ZEN 2011 software (ZEISS, Germany).

Table 2 provides instructions for identifying the twelve samples. The first letter of the label (A, B, C, or D) denotes the *marmorino* plaster formulation used for making the tile, the number (1, 2, or 3) specifies the finish layer employed, and the last character (p or c) indicates the fungal genera inoculated onto the surface.

For Scanning Electron Microscopy (SEM) analyses, a small sample was cut from the mock-up surface and affixed to the stub (sample holder) using conducting carbon cement. After drying, the sample was metalized with Chromium, and measurements were conducted. The SEM images were acquired using an FE-SEM (Field Emission Scanning Electron Microscopy) FEG LEO 1525 ZEISS, equipped with an in-lens detector for secondary electrons and operated at an accelerating voltage of 5 kV.

3.2.5. Photographs and micrographs interpretation

The interpretation of the naked eye observation was summarized considering the general development of the fungal colonization. Four levels were set and each sample was labeled with “extensively distributed”, “distributed”, “poorly distributed”, or “not appreciable” depending on how the Fungi were spread over the surface. It is important to underline that when the sample was labeled with “not appreciable” it could be related to the high efficiency of the antimicrobial system as well as to the limit of this kind of investigation.

Likewise, for the microscopy observation of the glass slides the following classification was assigned to the samples: considering both the presence of the conidia and the hyphae it was possible to define once again the fungal growth. Hence a rank system of five steps was generated: a Fungi with “high fungal growth” is when no obstacle in the fungal growth was observed; a “good fungal growth” was defined when both conidia and hyphal structures and at least one of them inside the matrix of the substrate can be seen; an “only superficial fungal growth” was assigned to the samples where the colonization was visible over the whole sample, but there was not penetration into the substrate; then a “not propagated/inhibited fungal growth” was given to the samples when the colonization was present only around the inoculation point or when a block on the development of the Fungi was identified; and finally a “not rooted fungal growth” was assigned when the fungal growth was totally inhibited.

As for the SEM images, the fungal colonization was evaluated through the observation of the spores and the hyphae’s characteristics (*i.e.*, amount, size, freshness, and distribution): *massive*, when pervious spores and hyphae of normal diameter/thickness were present, resulting in the mycelium being in an excellent vegetative state; *good*, when both pervious and dehydrated spores and hyphae of sufficient size were present; *sufficient*, when mostly dehydrated spores and hyphae were

present, although points of good rooting remained clearly visible in the mycelium; *regressed*, when only dehydrated, agglomerated, imploded spores and thin, dehydrated hyphae were visible.

4. Results

4.1. Fungi sampling campaign

From the sampling campaign conducted on the external walls of ancient palaces in the city of Venice presenting *marmorino* plaster in a discreet conservation state, it was possible to detect several Fungi species. *Penicillium italicum* (Fungi, Ascomicota, Eurotiales, Trichocomaceae) and *Cladosporium spherospermum* (Fungi Ascomycetes, Dothideomycetes, Cladosporiales) were then selected for this study, and their specific features are shown in Fig. 2S and Fig. 3S.

4.2. Photographic campaign and naked-eye observation

The results presented here pertain to pictures captured 30 days after the deposition of the Fungi inocula on the *marmorino* mock-ups, compared to those taken in the initial days following inoculation. The traditional *marmorino* tiles (mock-ups A) exhibited extensive

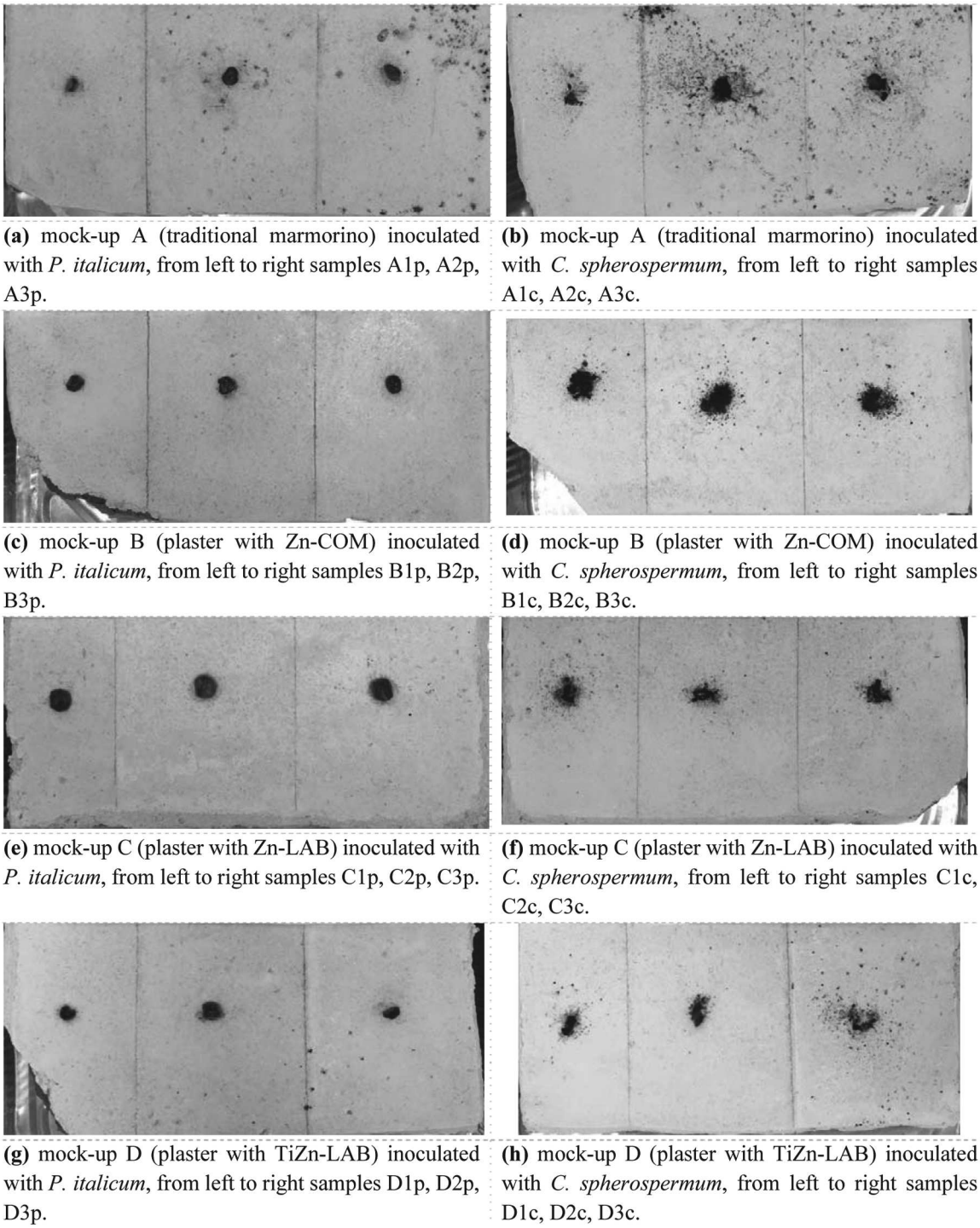

(a) mock-up A (traditional marmorino) inoculated with *P. italicum*, from left to right samples A1p, A2p, A3p.

(b) mock-up A (traditional marmorino) inoculated with *C. spherospermum*, from left to right samples A1c, A2c, A3c.

(c) mock-up B (plaster with Zn-COM) inoculated with *P. italicum*, from left to right samples B1p, B2p, B3p.

(d) mock-up B (plaster with Zn-COM) inoculated with *C. spherospermum*, from left to right samples B1c, B2c, B3c.

(e) mock-up C (plaster with Zn-LAB) inoculated with *P. italicum*, from left to right samples C1p, C2p, C3p.

(f) mock-up C (plaster with Zn-LAB) inoculated with *C. spherospermum*, from left to right samples C1c, C2c, C3c.

(g) mock-up D (plaster with TiZn-LAB) inoculated with *P. italicum*, from left to right samples D1p, D2p, D3p.

(h) mock-up D (plaster with TiZn-LAB) inoculated with *C. spherospermum*, from left to right samples D1c, D2c, D3c.

Fig. 1. : Photographs of the eight different marmorino tiles mock-ups colonized either by *P. italicum* or *C. spherospermum* Fungi.

microbiological colonization, noticeable even to the naked eye for both Fungi (Fig. 1 – a, b). Samples A2p, A3p, A2c, and A3c displayed widespread growth across the samples, indicating unhindered growth and diffusion of the microorganisms on the traditional substrate. In contrast, samples A1p and A1c exhibited less visible distributed fungal growth, likely due to the different bio-receptivity of the substrate. The more porous nature of the substrate may have facilitated the proximity of Fungi growth just to the inoculum area.

Furthermore, it should be noted that *Penicillium* sp. is greatly affected by pH, requiring an acidic environment between 3.0 and 4.5 for optimal development, although it is capable of taking root even in seemingly more adverse conditions. Conversely, *Cladosporium*, while tolerating acidic environments up to pH 4.4, needs an environment around pH 6.0 for optimal growth [70].

Similar trends were observed for mock-ups B and C. Both Fungi exhibited distinct interactions with the substrate. While *P. italicum* did not exhibit any visible growth on the tiles in any of the different finish layer options, *C. spherospermum* showed less dispersed colonization of the plaster in the case of Zn-LAB compared to the Zn-COM (Fig. 1 – c, d, e, f).

Finally, in the Ti-Zn-based tiles (mock-ups D), reduced growth of both *P. italicum* and *C. spherospermum* on the surfaces was observed. Additionally, the inoculum disk in the samples D3p and D3c (those with TiO_2 as finish layer) appeared to shrink or become not visible anymore (Fig. 1 – g, h).

These results are preliminary insights, but further analysis through optic and electronic microscopy is necessary to gain a more complete understanding of the interaction between the microorganisms and the different *marmorino* tiles.

4.3. Microscope investigation of the glass slides

Fig. 2 reports microscope investigations of glass slides from samples inoculated with the *Penicillium italicum* Fungus. In sample A1p, the presence of *P. italicum*'s conidia was evident in an ideal growth situation, although slightly smaller, often concatenated and intact; hyphae of the Fungus were also observed, but no conidiophore structures were present. Some contamination by external microorganisms, such as a cyanobacteria, likely originated from the environment where the tiles were stored, was noted.

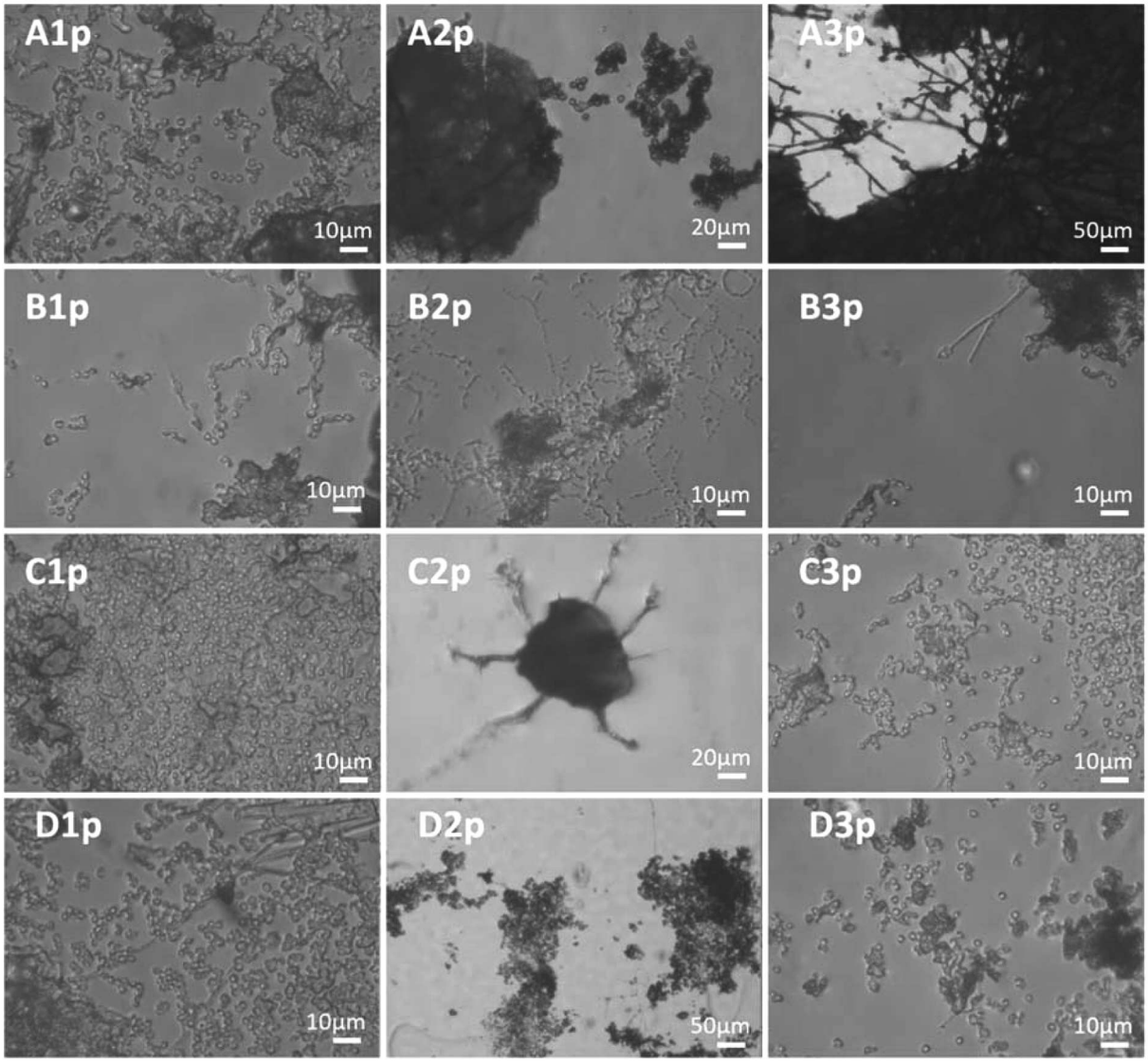

Fig. 2. : Microscopy pictures of (A) tile A Traditional *marmorino, (B)* tile B Zn-COM *marmorino,* (C) tile C Zn-LAB *marmorino,* (D) tile D ZnTi-LAB *marmorino,* inoculated with the *Penicillium italicum* Fungus. From left to write the samples with the three different finish layers: (1) no finish layer, (2) traditional Aleppo soap, and (3) Aleppo soap enriched with TiO_2 nanoparticles.

Sample A2p exhibited a Fungus in a good vegetative condition, with hyphae penetrating the *marmorino* matrix and intact chains of conidia visible. Additionally, biological consortium structures indicated the formation of a biofilm on the surface. Sample A3p showed a comparable situation to sample A2p, with slightly rounder and smaller conidia, and the presence of dry phialide structure with concatenated conidia nearby.

Regarding tile B inoculated with *P. italicum*, sample B1p revealed free conidia, sometimes still concatenated and dispersed in the plaster matrix, along with some hyphae exhibiting slight globular morphology, suggesting possible fungal growth deformation. Sample B2p also displayed a globular swelling structure and thin deformed hyphae penetrating the plaster matrix, with multiple inoculum points. In general, it was possible to notice very developed colonies in germination state with a young mycelium developed inside the matrix, with the uncommon presence of chlamydospores-like structures (*i.e.* thick-walled terminal or intercalary asexual resting propagule mostly for long-time survival) but already associated with *P. italicum* from some authors [71]; regarding the conidia, they were small and round, and concentrated near the inoculum area; it was also noticed an opaque surface, which might be linked to the presence of soap in the finish layer.

In sample B3p, filiform structures, likely underdeveloped hyphae, were observed. Performing an overview of the inoculum point and its vicinity, the conidia and the present hyphae were few, around 10–15 % compared to the previous glass slides; the observed conidia were still concatenated, but only present around the inoculum area, meaning that there was no growth, *i.e.* it could be potentially inhibited.

Sample C1p showed few fresh and some dry dehydrated hyphae, numerous conidia still concatenated covering the substrate, and cell structures resembling a flat coenobium. Sample C2p exhibited a small structured mycelium with hyphae penetrating the plaster matrix. Sample C3p displayed smaller chained spores only around the inoculation point.

In sample D1p, only the footprint of the mycelium structure and some dendriform structures (probably hyphae) were visible at the inoculation point, with limited fungal growth outside this area. A comparable scenario was observed in sample D2p, with vegetative body and sporulation structures present, but absent from the center of the inoculation point; in other parts of the glass slide, it was instead possible to notice conidiophores and thin hyphae, also inside the plaster structure. Sample D3p exhibited a thin conspicuous hyphal system confined

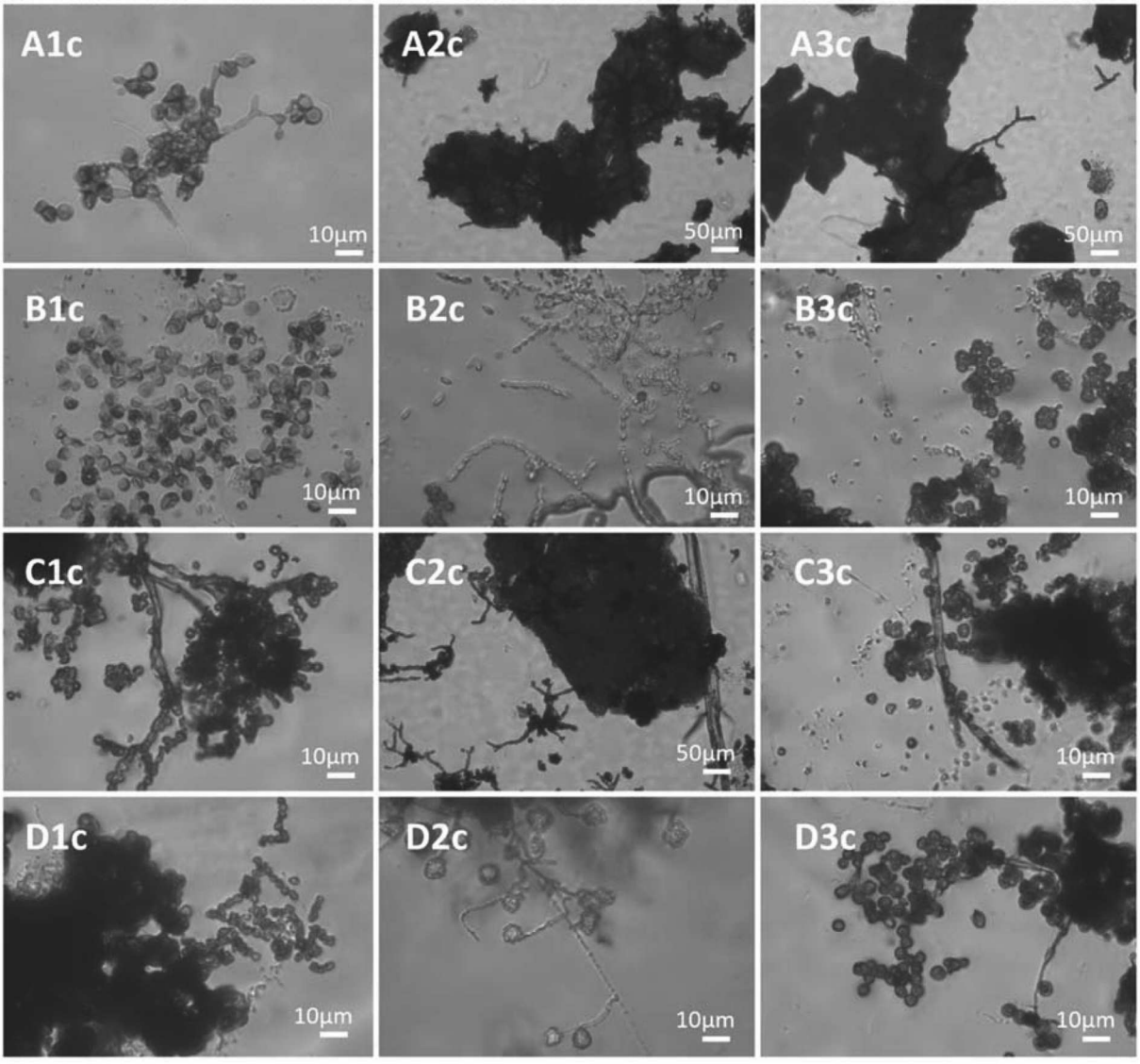

Fig. 3. : Microscopy pictures of (A) Tile A Traditional *marmorino, (B)* Tile B Zn-COM *marmorino,* (C) Tile C Zn-LAB *marmorino,* (D) Tile D ZnTi-LAB *marmorino,* inoculated with the *Cladosporium spherospermum* Fungus. From left to write the samples with the three different finish layers: (1) no finish layer, (2) traditional Aleppo soap, and (3) Aleppo soap enriched with TiO_2 nanoparticles.

to the surface and some dried conidiophores.

Regarding tile A inoculated with *Cladosporium spherospermum* (Fig. 3), in sample A1c the Fungus exhibited a conspicuous vegetative thallus, spreading across the glass slide, accompanied by numerous hyphae and conidia. Sample A2c displayed pieces of compacted mycelium once again, but smaller scattered conidia were absent. The Fungus managed to penetrate the plaster substrate, resulting in a higher presence of *marmorino* flakes adhered to the *Fungi-Tape*^{TM}. Sample A3c showcased an articulated-grained vegetative mycelium, with very few conidia present only in the inoculation point. The Fungus's growth appeared hindered, as the conidia seemed to have dried before sporulation.

In Sample B1c, a significant presence of small, mainly dehydrated conidia, and swollen broken hyphal cells was observed. Sample B2c exhibited fewer conidia than B1c, but more hyphae; the conidia were concentrated around the inoculation point, and hyphal systems were confined to this area, indicating limited propagation. A similar scenario was noted in sample B3c, with a compact but underdeveloped inoculum, as the Fungus did not propagate beyond the inoculation area. The conidia were dehydrated and unevenly arranged, and the mycelium was superficial and with thin hyphae.

In sample C1c, the Fungus presented subspherical scattered conidia, many of which were imploded, but no mycelium was visible. Conversely, in sample C2c, it appeared that the Fungus had initially taken root but then receded from the substrate, as evidenced by imploded and attached conidia, very thin hyphae, and a mycelium with short hyphal cells. Sample C3c showed no apparent root formation by the Fungus, since there is no mycelium present, with only a few thick hyphae and singularly scattered imploded small conidia, although fewer than in C2c.

Sample D1c displayed a densely compacted mycelium, but the Fungus was limited to the surface, with small and dehydrated conidia and hyphae exhibiting shorter cells. In sample D2c, the Fungus appeared mostly dehydrated, with interrupted growth phases of the mycelium, and sporulating elements with very small conidia were also visible. Finally, in sample D3c, a dehydrated Fungus with a developed mycelium was observed, primarily with hyphal forms over the matrix surface but not within, along with collapsed or imploded small conidia showing

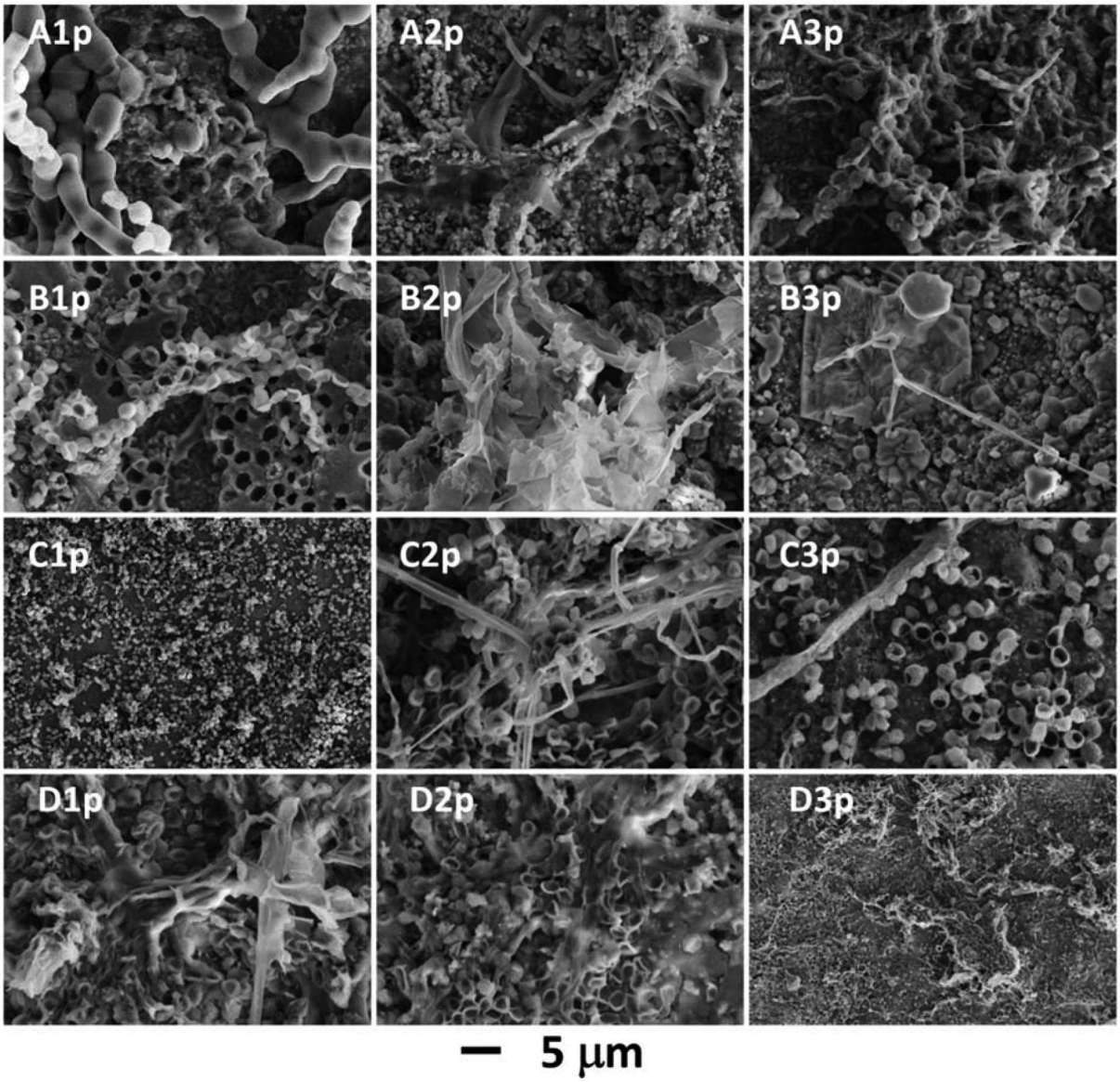

Fig. 4. : SEM images of (A) Tile A Traditional *marmorino, (B)* Tile B Zn-COM *marmorino,* (C) Tile C Zn-LAB *marmorino,* (D) Tile D ZnTi-LAB *marmorino,* inoculated with the *Penicillium italicum* Fungus. From left to write the samples with the three different finish layers: (1) no finish layer, (2) traditional Aleppo soap, and (3) Aleppo soap enriched with TiO_2 nanoparticles.

evident cavities. Some residual network structures, likely residual conidiophores, were also noted.

4.4. Scanning electron microscopy analyses

Scanning Electron Microscopy (SEM) proved to be a valuable technique for detailed examination of fungal growth across the various samples. Particular attention was focused towards assessing the presence and distribution of spores and hyphae on the surface, their morphological characteristics, and their condition.

Regarding the *Penicillium italicum* Fungus (Fig. 4), sample A1p exhibits thick globular phialides and a high concentration of spores distributed on the surface. In sample A2p, hyphae were observed scattered across the surface along with some dried spores. Additionally, irregular grains were noted over the *P. italicum* Fungus, potentially indicating substrate alteration caused by the Fungus. Images from sample A3p depicted short and thick hyphae along with some characteristic concatenated spores, most of which appeared dried and exhibited shape deformations.

Sample B1p showcased a surface highly colonized by *P. italicum*, featuring chains of spores and thin, elongated hyphae. Notably, a compact layer with perforation was observed, indicating the presence of *P. italicum* colonies both underneath and atop it. Conversely, in sample B2p, a scarce distribution of spores was observed, except near the inoculation point. Additionally, a transparent-whiteish element resembling an agglomeration of really dried and broken hyphae that create a cloth-like effect, likely due to Aleppo soap finish layer, was noted. Similarly, sample B3p exhibited a modest presence of spores and hyphae, primarily around the inoculation site.

In sample C1p, a significant number of smaller spores and dried hyphae were observed, although with a non-homogenous distribution on the surface, suggesting uneven growth. Sample C2p displayed small, occasionally agglomerated spores, and dried, elongated hyphae. Conversely, in sample C3p, both the number of hyphae and spores were lower, with spores appearing small and sufficiently dry to fracture.

Sample D1p presented a high density of spores homogeneously

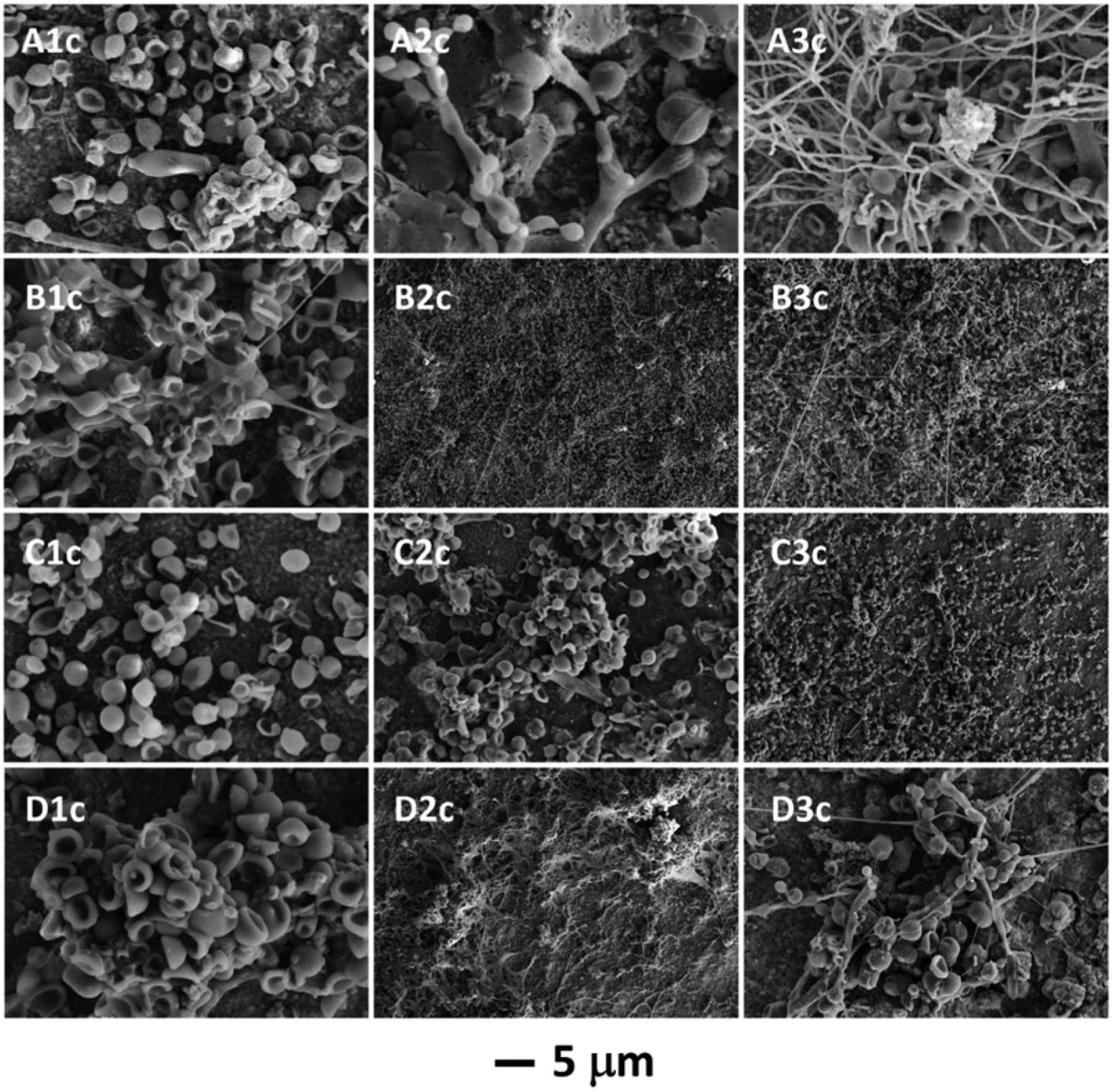

Fig. 5. : SEM images of (A) Tile A Traditional *marmorino, (B)* Tile B Zn-COM *marmorino,* (C) Tile C Zn-LAB *marmorino,* (D) Tile D ZnTi-LAB *marmorino,* inoculated with the *Cladosporium spherospermum* Fungus. From left to write the samples with the three different finish layers: (1) no finish layer, (2) traditional Aleppo soap, and (3) Aleppo soap enriched with TiO_2 nanoparticles.

distributed on the surface, while hyphae were scarce, dried, and fragmented, forming a flake-like structure. In sample D2p, small spores embedded in a mucilaginous-like structure were visible, possibly associated with Aleppo soap agglomerations or a densely compact hyphal network. Finally, sample D3p finally exhibited a small quantity of dry, agglomerated spores along with long, thin, and dried hyphae.

Regarding the *marmorino* mock-up tiles colonized by *Cladosporium spherospermum* (Fig. 5), a situation similar to that described for the *Penicillium italicum* colonization was observed. On sample A1c, fungal spores of various dimensions and hyphae were visible, distributed over the surface. In sample A2c, ramoconidia were once again observed, along with hyphae. Notably, spherical structures suggestive of spores in germination were present. In sample A3c, there was a generally significant decrease in the number of spores, which appeared deformed, with only few very thin hyphae visible. It is also interesting to note the presence of crystals probably directly produced by the Fungus [72].

In sample B1c, a high concentration of spores was evident, with surficial hyphae indicating a developed mycelium that subsequently dried up. Sample B2c exhibited conglomerates of dry spores, small spores, and really elongated hyphal systems. In sample B3c, dry spores conglomerates were again present, although smaller in size, with a general decrease in pore size. Long and dry hyphal structures were also visible.

Sample C1c displayed equally dispersed small spores but no evidence of hyphal network. Similarly, in sample C2c, small spores were present without long hyphae, but hyphal cells were observed. Likewise, in sample C3c, the absence of hyphae and the presence of small drier spores were notable.

In sample D1c, conglomerates of imploded, dry, medium-sized spores were unevenly distributed on the surface, with no visible hyphae. In sample D2c, spores of varying dimensions were observed, inserted in a mucilaginous-like structure, as seen in the *P. italicum* inoculation in sample D2p. Finally, in sample D3c, conglomerates of smaller and larger spores were present.

5. Discussion

To better deal with the high amount of results, mainly based on image interpretation, the parameters taken into account were summarized, as described in paragraph 3.2.5, and were used to design Table 3. In this way, it was possible to show the results and efficiently underline the effect of the synergetic combination of photocatalysts in contrasting the biodeterioration on the *marmorino* plaster mock-ups.

Investigating the effect of the different photocatalysts, it was observed that the incorporation of ZnO in the plaster mixture, as well as the enrichment with TiO_2 in the finish layer, generally endowed the plaster with antimicrobial features or hindered fungal proliferation in some extent.

Specifically, in the case of Zn-base materials in the plaster mixture, better results were obtained with laboratory-made photocatalysts. This correlation can be attributed to the photoactivity of zinc oxides; all the three samples present optoelectronic properties which were correlated with their activity, resulting in an increasing level of activity from Zn-COM, to Zn-LAB, and finally to ZnTi-LAB, as it has been previously demonstrated by the authors [48,50]. In Zn-COM and Zn-LAB *marmorino*, Zn–OH surface groups delay photoactivity by trapping photoexcited charge carriers on the hydroxyl group, thereby diminishing activity by insulation and acting as an electrical barrier for charge transfer. On the other hand, in ZnTi-LAB, the passivation of Zn–OH surface groups and the increased number of heterojunctions enhance the activity by reducing the excited states quench, thereby implementing charge separation [73,74].

Furthermore, it was previously observed that the Zn-COM sample exhibited a $Ca(OH)_2$-rich surface, which could act as insulating layer, reducing free radical production and thereby limiting a potential way to arm the biological proliferation. The ZnTi-LAB nanomaterial, comprising a zinc oxide core and a titanium dioxide shell, previously demonstrated the most effective self-bleaching activity due to enhanced heterojunction formation among the photoactive phases [48]. For the same reasons, a higher arming interaction with the biological materials could explain the obtained superior results.

In absence of finish layer, the susceptibility to biological attacks is heightened. Applying a finish layer reduces surface bio-receptivity by reducing available pores. However, it is important to note that while surface hydrophobicity increases with the application of soap, applying organic material on an already carbonated plaster surface could serve as metabolic source for microorganisms. This could explain the microbial proliferation in samples treated with Aleppo soap finish layer.

Table 3
Summary of the obtained results.

***Marmorino* plaster mixture**	**Finish layer**	**Sample**	**Naked-eye observation (colonization level)**	**Microscope glass-slide (fungal growth)**	**SEM images**
Traditional	No finish layer	A1p	Not appreciable	High	massive
		A1c	Not appreciable	High	massive
	Traditional (Aleppo soap)	A2p	Extensively distributed	Good	good
		A2c	Extensively distributed	Good	massive
	Aleppo soap + TiO_2	A3p	Extensively distributed	Good	sufficient
		A3c	Extensively distributed	Inhibited/not propagated	good
Enriched with Zn-COM	No finish layer	B1p	Not appreciable	Good	good
		B1c	Distributed	High	good
	Traditional (Aleppo soap)	B2p	Not appreciable	Good	good
		B2c	Distributed	Inhibited/not propagated	sufficient
	Aleppo soap + TiO_2	B3p	Not appreciable	Inhibited/not propagated	regressed
		B3c	Distributed	Inhibited/not propagated	regressed
Enriched with Zn-LAB	No finish layer	C1p	Not appreciable	Only superficial	sufficient
		C1c	Poorly distributed	Only superficial	good/ sufficient
	Traditional (Aleppo soap)	C2p	Not appreciable	Good	sufficient
		C2c	Poorly distributed	Inhibited/not propagated	good/ sufficient
	Aleppo soap + TiO_2	C3p	Not appreciable	Inhibited/not propagated	regressed
		C3c	Poorly distributed	Not rooted	regressed
Enriched with ZnTi-LAB	No finish layer	D1p	Poorly distributed	Inhibited/not propagated	sufficient
		D1c	Poorly distributed	Only superficial	sufficient
	Traditional (Aleppo soap)	D2p	Poorly distributed	Inhibited/not propagated	regressed
		D2c	Poorly distributed	Inhibited/not propagated	regressed
	Aleppo soap + TiO_2	D3p	Poorly distributed	Only superficial	sufficient
		D3c	Poorly distributed	Inhibited/not propagated	sufficient/ regressed

On the other hand, adding TiO_2 NPs to Aleppo soap resulted in improved antimicrobial effects, inhibiting or even preventing microbiological colonization in most cases. This confirms the antimicrobial features of TiO_2, which are mainly attributed to the generation of free radicals that compromise the structural and functional integrity of microorganism cells, ultimately leading to pathogenic cell death or significant reduction in growth and proliferation.

Moreover, the chemical and electrical features of TiO_2 contribute to its antimicrobic action. Its good electric conductivity can damage cell membranes and inhibit metabolic pathways, thereby reducing the ability of microorganisms to obtain energy and nutrients for reproduction, including spore germination and the formation of new fungal colonies [75,76]. This aspect is particularly emphasized in the samples containing metal oxides in both in the plaster mixture and finish layer, creating a hostile environment for microbiological proliferation through a synergetic effect.

6. Conclusions

This study investigated the antimicrobial properties of TiO_2 and ZnO against two Fungi, *Penicillium italicum* and *Cladosporium spherospermum*, directly sampled from real-case scenarios. The photocatalysts were incorporated into the formulation of Venetian traditional *marmorino*, with different finish layers, allowing for a comparison between a traditional layer of Aleppo soap and innovative TiO_2-based one.

For both Fungi, the presence of zinc oxides in the plaster mixture helped create an unfavorable environment for fungal proliferation. the best results were obtained with the lab-made ZnTi-LAB. Regarding the finish layer, the addition of TiO_2 to Aleppo soap increased the antimicrobic effect, strengthening the surface's ability to contrast fungal growth. Given the intrinsic features of the two metals oxides, their antimicrobial activity was correlated with their photocatalytic and optoelectrical properties.

In conclusion, this study demonstrated the feasibility of conferring antimicrobial properties to Venetian *marmorino* plaster through the use of photocatalysts, effectively merging historical traditional materials with scientific innovation.

Declaration of Competing Interest

The authors declare that they have no known competing financial interests or personal relationships that could have appeared to influence the work reported in this paper.

Acknowledgments

The authors would like to thank Mr. Giorgio Berto and Arch. Guido Jaccarino (Uni.S.Ve. s.r.l., Venice, Italy) and Arch. Luca Scappin (I.U.A.V. University of Venice, Venice, Italy) for their collaboration and technical assistance with the *marmorino* plaster tiles preparation and historical background. Furthermore, we would like to acknowledge Ms. Elisa Lanaro for her practical contributions to this work. Andrea Campostrini finally thanks the "PON Ricerca e Innovazione 2014–2020" and "Fondo per la promozione e lo sviluppo delle politiche del Programma Nazionale per la Ricerca (PNR) 2021–2027" for financing his Ph.D. scholarship.

Appendix A. Supporting information

Supplementary data associated with this article can be found in the online version at doi:10.1016/j.nxmate.2024.100384.

References

[1] F. Izzo, A. Arizzi, P. Cappelletti, G. Cultrone, A. De Bonis, C. Germinario, S. F. Graziano, C. Grifa, V. Guarino, M. Mercurio, V. Morra, A. Langella, The art of building in the Roman period (89 B.C. – 79 A.D.): Mortars, plasters and mosaic floors from ancient Stabiae (Naples, Italy), Constr. Build. Mater. 117 (2016) 129–143, https://doi.org/10.1016/J.CONBUILDMAT.2016.04.101.
[2] M. Mogetta, The Origins of Concrete Construction in Roman Architecture, Cambridge University Press, 2021, https://doi.org/10.1017/9781108990516.
[3] N. Huse, W. Wolters, The art of renaissance Venice: architecture, sculpture, and painting, 1460-1590, 29-0081-29–0081, Choice Rev. Online 29 (1991), https://doi.org/10.5860/CHOICE.29-0081.
[4] R. Berto, A. Prà, S.P. Maffei, P. Rosato, The appraisal of reproduction costs of historic properties: the case of Venetian Villas / La stima del costo di riproduzione delle dimore storiche: il caso delle Ville Venete, Valor e Valuta 30 (2022) 45–58, https://doi.org/10.48264/VVSIEV-20223003.
[5] D. Howard, Four centuries of literature on palladio, J. Soc. Archit. Hist. 39 (1980) 224–241, https://doi.org/10.2307/989568.
[6] M. Caroselli, S.A. Ruffolo, F. Piqué, Mortars and plasters—how to manage mortars and plasters conservation, Archaeol. Anthr. Sci. 13 (2021) 188, https://doi.org/10.1007/s12520-021-01409-x.
[7] A. Squassina, Construction wisdom: preserving venice with both tradition and innovation, Stud. Conserv. 67 (2022) 253–259, https://doi.org/10.1080/00393630.2022.2046413.
[8] A. Ferrighi, The plaster catalogue: comments on the result of the research, Catalogue of Venetian Plasters and Historical Interventions for High Water Defense (2006).
[9] R. Piovesan, R. Siddall, C. Mazzoli, L. Nodari, The Temple of Venus (Pompeii): a study of the pigments and painting techniques, J. Archaeol. Sci. 38 (2011) 2633–2643, https://doi.org/10.1016/J.JAS.2011.05.021.
[10] A. Remotto, E. Balliana, F.C. Izzo, G. Biscontin, E. Zendri, Regalzier: study of a typical historical plaster finish in Venice, Conserv. Sci. Cult. Herit. 12 (2012) 309–327, https://doi.org/10.6092/ISSN.1973-9494/3402.
[11] F. Trovo', E. Vettore, The role of craftsmanship in the conservation of Venice. State of the art and perspective. Proceedings HERITAGE 2022 - International Conference on Vernacular Heritage: Culture, People and Sustainability, Universitat Politècnica de València, Valencia, 2022, pp. 1–9, https://doi.org/10.4995/HERITAGE2022.2022.15690.
[12] N. Tsui, R.J. Flatt, G.W. Scherer, Crystallization damage by sodium sulfate, J. Cult. Herit. 4 (2003) 109–115, https://doi.org/10.1016/S1296-2074(03)00022-0.
[13] D. De la Fuente, J.M. Vega, F. Viejo, I. Díaz, M. Morcillo, Mapping air pollution effects on atmospheric degradation of cultural heritage, J. Cult. Herit. 14 (2013) 138–145, https://doi.org/10.1016/J.CULHER.2012.05.002.
[14] P. Maravelaki-Kalaitzaki, G. Biscontin, Origin, characteristics and morphology of weathering crusts on Istria stone in Venice, Atmos. Environ. 33 (1999) 1699–1709, https://doi.org/10.1016/S1352-2310(98)00263-5.
[15] B.J. Smith, M. Gomez-Heras, S. McCabe, Understanding the decay of stone-built cultural heritage, Prog. Phys. Geogr.: Earth Environ. 32 (2008) 439–461, https://doi.org/10.1177/0309133308098119.
[16] I. Costantini, J. Aramendia, E. Tomasini, K. Castro, J. Manuel Madariaga, G. Arana, Detection of unexpected copper sulfate decay compounds on late Gothic mural paintings: assessing the threat of environmental impact, Microchem. J. 169 (2021) 106542, https://doi.org/10.1016/J.MICROC.2021.106542.
[17] V. Fassina, M. Favaro, A. Naccari, M. Pigo, Evaluation of compatibility and durability of a hydraulic lime-based plaster applied on brick wall masonry of historical buildings affected by rising damp phenomena, J. Cult. Herit. 3 (2002) 45–51, https://doi.org/10.1016/S1296-2074(02)01158-5.
[18] G. Leone, A. De Vita, A. Magnani, C. Rossi, Thermal and petrographic characterization of herculaneum wall plasters, Archaeometry 59 (2017) 747–761, https://doi.org/10.1111/arcm.12275.
[19] D. Ergenç, R. Fort, M.J. Varas−Muriel, M. Alvarez de Buergo, Mortars and plasters—how to characterize aerial mortars and plasters, Archaeol. Anthr. Sci. 13 (2021) 197, https://doi.org/10.1007/s12520-021-01398-x.
[20] E. Guolo, P. Romagnoni, F. Peron, Capillary rising damp in Venetian context: state of the art and numerical simulation, J. Phys. Conf. Ser. 2069 (2021) 012046, https://doi.org/10.1088/1742-6596/2069/1/012046.
[21] E. Sesana, A.S. Gagnon, C. Ciantelli, J. Cassar, J.J. Hughes, Climate change impacts on cultural heritage: a literature review, WIREs Clim. Change 12 (2021), https://doi.org/10.1002/wcc.710.
[22] C. Rodriguez-Navarro, E. Sebastian, Role of particulate matter from vehicle exhaust on porous building stones (limestone) sulfation, Sci. Total Environ. 187 (1996) 79–91, https://doi.org/10.1016/0048-9697(96)05124-8.
[23] L. Falchi, E. Orio, E. Balliana, F.C. Izzo, E. Zendri, Investigation on the relationship between the environment and istria stone surfaces in Venice, Atmos. Environ. 210 (2019) 76–85, https://doi.org/10.1016/J.ATMOSENV.2019.04.044.
[24] P.S. Griffin, N. Indictor, R.J. Koestler, The biodeterioration of stone: a review of deterioration mechanisms, conservation case histories, and treatment, Int. Biodeterior. 28 (1991) 187–207, https://doi.org/10.1016/0265-3036(91)90042-P.
[25] A. Mihajlovski, D. Seyer, H. Benamara, F. Bousta, P. Di Martino, An overview of techniques for the characterization and quantification of microbial colonization on stone monuments, Ann. Microbiol. 65 (2015) 1243–1255, https://doi.org/10.1007/s13213-014-0956-2.
[26] T.C. Dakal, S.S. Cameotra, Microbially induced deterioration of architectural heritages: routes and mechanisms involved, Environ. Sci. Eur. 24 (2012) 36, https://doi.org/10.1186/2190-4715-24-36.
[27] E. Stanaszek-Tomal, Environmental factors causing the development of microorganisms on the surfaces of national cultural monuments made of mineral building materials—review, Coatings 10 (2020) 1203, https://doi.org/10.3390/coatings10121203.

[28] C. Sabbioni, A. Bonazza, G. Zappia, Damage on hydraulic mortars: the Venice Arsenal, J. Cult. Herit. 3 (2002) 83–88, https://doi.org/10.1016/S1296-2074(02)01163-9.

[29] T. Warscheid, J. Braams, Biodeterioration of stone: a review, Int. Biodeterior. Biodegrad. 46 (2000) 343–368, https://doi.org/10.1016/S0964-8305(00)00109-8.

[30] K. Sterflinger, Fungi: their role in deterioration of cultural heritage, Fungal Biol. Rev. 24 (2010) 47–55, https://doi.org/10.1016/J.FBR.2010.03.003.

[31] F. De Leo, A. Marchetta, C. Urzì, Black fungi on stone-built heritage: current knowledge and future outlook, Appl. Sci. 12 (2022) 3969, https://doi.org/10.3390/app12083969.

[32] M.L. Coutinho, A.Z. Miller, M.F. Macedo, Biological colonization and biodeterioration of architectural ceramic materials: an overview, J. Cult. Herit. 16 (2015) 759–777, https://doi.org/10.1016/j.culher.2015.01.006.

[33] L. Schröer, N. Boon, T. De Kock, V. Cnudde, The capabilities of bacteria and archaea to alter natural building stones – a review, Int. Biodeterior. Biodegrad. 165 (2021) 105329, https://doi.org/10.1016/J.IBIOD.2021.105329.

[34] X. Liu, Y. Qian, F. Wu, Y. Wang, W. Wang, J.D. Gu, Biofilms on stone monuments: biodeterioration or bioprotection? Trends Microbiol. 30 (2022) 816–819, https://doi.org/10.1016/J.TIM.2022.05.012.

[35] A. Negi, I.P. Sarethy, Microbial biodeterioration of cultural heritage: events, colonization, and analyses, Micro Ecol. 78 (2019) 1014–1029, https://doi.org/10.1007/s00248-019-01366-y.

[36] E. Gioventù, P. Lorenzi, Bio-removal of black crust from marble surface: comparison with traditional methodologies and application on a sculpture from the Florence's English cemetery, Procedia Chem. 8 (2013) 123–129, https://doi.org/10.1016/J.PROCHE.2013.03.017.

[37] S. Pozo, P. Barreiro, T. Rivas, P. González, M.P. Fiorucci, Effectiveness and harmful effects of removal sulphated black crust from granite using Nd:YAG nanosecond pulsed laser, Appl. Surf. Sci. 302 (2014) 309–313, https://doi.org/10.1016/J.APSUSC.2013.10.129.

[38] C. Ricci, F. Gambino, M. Nervo, A. Piccirillo, A. Scarcella, F. Zenucchini, A. Ramil, J.S. Pozo-Antonio, Enhancement of graffiti removal from heritage stone by combining laser ablation and application of a solvent mixture, Constr. Build. Mater. 262 (2020) 119934, https://doi.org/10.1016/J.CONBUILDMAT.2020.119934.

[39] S.A. Ruffolo, M.F. La Russa, Nanostructured coatings for stone protection: an overview, Front. Mater. 6 (2019), https://doi.org/10.3389/fmats.2019.00147.

[40] S.K. Kirthika, G. Goel, A. Matthews, S. Goel, Review of the untapped potentials of antimicrobial materials in the construction sector, Prog. Mater. Sci. 133 (2023), https://doi.org/10.1016/j.pmatsci.2022.101065.

[41] L. Liao, M. Wang, Z. Li, X. Wang, W. Zhou, Recent advances in black TiO2 nanomaterials for solar energy conversion, Nanomaterials 13 (2023) 468, https://doi.org/10.3390/nano13030468.

[42] N. Madkhali, C. Prasad, K. Malkappa, H.Y. Choi, V. Govinda, I. Bahadur, R. A. Abumousa, Recent update on photocatalytic degradation of pollutants in waste water using TiO2-based heterostructured materials, Results Eng. 17 (2023) 100920, https://doi.org/10.1016/J.RINENG.2023.100920.

[43] A. Bathla, S.A. Younis, K.-H. Kim, X. Li, TiO2-based catalytic systems for the treatment of airborne aromatic hydrocarbons, Mater. Horiz. (2023), https://doi.org/10.1039/D2MH01583H.

[44] S. Veltri, A.M. Palermo, G. De Filpo, F. Xu, Subsurface treatment of TiO2 nanoparticles for limestone: prolonged surface photocatalytic biocidal activities, Build. Environ. 149 (2019) 655–661, https://doi.org/10.1016/J.BUILDENV.2018.10.038.

[45] I. Alfieri, A. Lorenzi, L. Ranzenigo, L. Lazzarini, G. Predieri, P.P. Lottici, Synthesis and characterization of photocatalytic hydrophobic hybrid TiO2-SiO2 coatings for building applications, Build. Environ. 111 (2017) 72–79, https://doi.org/10.1016/J.BUILDENV.2016.10.019.

[46] N. Gómez-Ortíz, S. De la Rosa-García, W. González-Gómez, M. Soria-Castro, P. Quintana, G. Oskam, B. Ortega-Morales, Antifungal coatings based on $Ca(OH)_2$ mixed with ZnO/TiO_2 nanomaterials for protection of limestone monuments, ACS Appl. Mater. Interfaces 5 (2013) 1556–1565, https://doi.org/10.1021/am302783h.

[47] M.F. La Russa, A. Macchia, S.A. Ruffolo, F. De Leo, M. Barberio, P. Barone, G. M. Crisci, C. Urzì, Testing the antibacterial activity of doped TiO2 for preventing biodeterioration of cultural heritage building materials, Int. Biodeterior. Biodegrad. 96 (2014) 87–96, https://doi.org/10.1016/J.IBIOD.2014.10.002.

[48] D. Zanardo, E. Ghedini, F. Menegazzo, A. Giordana, G. Cerrato, A.Di Michele, G. Cruciani, M. Signoretto, Traditional Venetian marmorino: effect of zinc-based oxides on self-bleaching properties, J. Cult. Herit. 50 (2021) 171–178, https://doi.org/10.1016/J.CULHER.2021.04.006.

[49] M. Dell'Edera, C. Lo Porto, I. De Pasquale, F. Petronella, M.L. Curri, A. Agostiano, R. Comparelli, Photocatalytic TiO2-based coatings for environmental applications, Catal. Today 380 (2021) 62–83, https://doi.org/10.1016/J.CATTOD.2021.04.023.

[50] L. Scappin, A. Campostrini, D. Zanardo, E. Ghedini, M. Signoretto, G. Berto, F. Menegazzo, Marmorino and photocatalysts: a meeting between tradition and innovation, Int. J. Arch. Conserv. Restor. I (2022) 35–49, https://doi.org/10.57639/SIRA.INTR0104.

[51] H. Shu, M. Yang, Q. Liu, M. Luo, Study of TiO2-modified sol coating material in the protection of stone-built cultural heritage, Coatings 10 (2020) 179, https://doi.org/10.3390/coatings10020179.

[52] F. Gherardi, A. Colombo, M. D'Arienzo, B. Di Credico, S. Goidanich, F. Morazzoni, R. Simonutti, L. Toniolo, Efficient self-cleaning treatments for built heritage based on highly photo-active and well-dispersible TiO2 nanocrystals, Microchem. J. 126 (2016) 54–62, https://doi.org/10.1016/j.microc.2015.11.043.

[53] N. Ditaranto, I.D. van der Werf, R.A. Picca, M.C. Sportelli, L.C. Giannossa, E. Bonerba, G. Tantillo, L. Sabbatini, Characterization and behaviour of ZnO-based nanocomposites designed for the control of biodeterioration of patrimonial stoneworks, N. J. Chem. 39 (2015) 6836–6843, https://doi.org/10.1039/C5NJ00527B.

[54] J.D. Bersch, I. Flores-Colen, A.B. Masuero, D.C.C. Dal Molin, Photocatalytic TiO2-based coatings for mortars on facades: a review of efficiency, durability, and sustainability, Buildings 13 (2023), https://doi.org/10.3390/buildings13010186.

[55] G.M.C. Gemelli, M. Luna, R. Zarzuela, M.L.A. Gil Montero, M. Carbú, I. Moreno-Garrido, M.J. Mosquera, 4-Year in-situ assessment of a photocatalytic TiO2/SiO2 antifouling treatment for historic mortar in a coastal city, Build. Environ. 225 (2022) 109627, https://doi.org/10.1016/j.buildenv.2022.109627.

[56] S. Veltri, A.M. Palermo, G. De Filpo, F. Xu, Subsurface treatment of TiO2 nanoparticles for limestone: prolonged surface photocatalytic biocidal activities, Build. Environ. 149 (2019) 655–661, https://doi.org/10.1016/j.buildenv.2018.10.038.

[57] G.B. Goffredo, S. Accoroni, C. Totti, T. Romagnoli, L. Valentini, P. Munafò, Titanium dioxide based nanotreatments to inhibit microalgal fouling on building stone surfaces, Build. Environ. 112 (2017) 209–222, https://doi.org/10.1016/j.buildenv.2016.11.034.

[58] A. Sierra-Fernandez, S.C. De la Rosa-García, L.S. Gomez-Villalba, S. Gómez-Cornelio, M.E. Rabanal, R. Fort, P. Quintana, Synthesis, photocatalytic, and antifungal properties of MgO, ZnO and Zn/Mg oxide nanoparticles for the protection of calcareous stone heritage, ACS Appl. Mater. Interfaces 9 (2017) 24873–24886, https://doi.org/10.1021/acsami.7b06130.

[59] K. Loh, C.C. Gaylarde, M.A. Shirakawa, Photocatalytic activity of ZnO and TiO2 'nanoparticles' for use in cement mixes, Constr. Build. Mater. 167 (2018) 853–859, https://doi.org/10.1016/j.conbuildmat.2018.02.103.

[60] M. Abd Elgaleel Hossin, T.M. Tiama, A. Hussein, A. Russlan, The anti-bacterial lime mortar used in the restoration of ancient limestone buildings by adding heavy metal oxide, Int. J. Multidiscip. Stud. Archit. Cult. Herit. 5 (2022) 93–122, https://doi.org/10.21608/ijmsac.2022.276737.

[61] M.M. Khan, M.H. Harunsani, A.L. Tan, M. Hojamberdiev, Y.A. Poi, N. Ahmad, Antibacterial studies of ZnO and Cu-doped ZnO nanoparticles synthesized using aqueous leaf extract of Stachytarpheta jamaicensis, Bionanoscience 10 (2020) 1037–1048, https://doi.org/10.1007/s12668-020-00775-5.

[62] S. Gunalan, R. Sivaraj, V. Rajendran, Green synthesized ZnO nanoparticles against bacterial and fungal pathogens, Prog. Nat. Sci.: Mater. Int. 22 (2012) 693–700, https://doi.org/10.1016/j.pnsc.2012.11.015.

[63] J. Sawai, Quantitative evaluation of antibacterial activities of metallic oxide powders (ZnO, MgO and CaO) by conductimetric assay, J. Microbiol. Methods 54 (2003) 177–182, https://doi.org/10.1016/S0167-7012(03)00037-X.

[64] N. Jones, B. Ray, K.T. Ranjit, A.C. Manna, Antibacterial activity of ZnO nanoparticle suspensions on a broad spectrum of microorganisms, FEMS Microbiol. Lett. 279 (2008) 71–76, https://doi.org/10.1111/j.1574-6968.2007.01012.x.

[65] I. Klapiszewska, A. Kubiak, A. Parus, M. Janczarek, A. Ślosarczyk, The in situ hydrothermal and microwave syntheses of zinc oxides for functional cement composites, Materials 15 (2022), https://doi.org/10.3390/ma15031069.

[66] V. Trevisan, M. Signoretto, F. Pinna, G. Cruciani, G. Cerrato, Investigation on titania synthesis for photocatalytic NOx abatement, Chem. Today 30 (2012) 25–28.

[67] D. Zanardo, G. Forghieri, E. Ghedini, F. Menegazzo, A. Giordana, G. Cerrato, E. Cattaruzza, A. Di Michele, G. Cruciani, M. Signoretto, Effect of the synthetic parameters over ZnO in the CO2 photoreduction, Molecules 28 (2023) 4798, https://doi.org/10.3390/molecules28124798.

[68] R.A. Samson, J. Houbraken, U. Thrane, J.C. Frisvad, B. Andersen, Food and Indoor Fungi, CBS-KNAW Fungal Biodiversity Centre, Utrecht, 2010.

[69] D. Sharma, J. Rajput, B.S. Kaith, M. Kaur, S. Sharma, Synthesis of ZnO nanoparticles and study of their antibacterial and antifungal properties, Thin Solid Films 519 (2010) 1224–1229, https://doi.org/10.1016/j.tsf.2010.08.073.

[70] M.A. Shirakawa, I.B. Beech, R. Tapper, M.A. Cincotto, W. Gambale, The development of a method to evaluate bioreceptivity of indoor mortar plastering to fungal growth, Int Biodeterior. Biodegrad. 51 (2003) 83–92, https://doi.org/10.1016/S0964-8305(01)00129-9.

[71] J.E. Spraker, L.M. Sanchez, T.M. Lowe, P.C. Dorrestein, N.P. Keller, Ralstonia solanacearum lipopeptide induces chlamydospore development in fungi and facilitates bacterial entry into fungal tissues, ISME J. 10 (2016) 2317–2330, https://doi.org/10.1038/ismej.2016.32.

[72] A. Micheluz, F. Pinzari, E.G. Rivera-Valentín, S. Manente, J.E. Hallsworth, Biophysical manipulation of the extracellular environment by Eeurotium halophilicum, Pathogens 11 (2022) 1462, https://doi.org/10.3390/pathogens11121462.

[73] T.-C. Lin, M.Y.A. Mollah, R.K. Vempati, D.L. Cocke, Synthesis and characterization of calcium hydroxyzincate using X-ray diffraction, FT-IR spectroscopy, and scanning force microscopy, Chem. Mater. 7 (1995) 1974–1978, https://doi.org/10.1021/cm00058a031.

[74] K. KOBAYAKAWA, Y. NAKAZAWA, M. IKEDA, Y. SATO, A. FUJISHIMA, ChemInform abstract: influence of the density of surface hydroxyl groups on tio2

photocatalytic activities, ChemInform 22 (1991), https://doi.org/10.1002/chin.199112023.

[75] A. Fouda, M. Abdel-Nasser, A.M. Eid, S.E.-D. Hassan, A. Abdel-Nasser, N. K. Alharbi, A.H. AlRokban, G. Abdel-Maksoud, An eco-friendly approach utilizing green synthesized titanium dioxide nanoparticles for leather conservation against a fungal strain, Penicillium expansum AL1, Involved in the biodeterioration of a historical manuscript, Biology (Basel) 12 (2023) 1025, https://doi.org/10.3390/biology12071025.

[76] S. Park, S. Lee, B. Kim, S. Lee, J. Lee, S. Sim, M. Gu, J. Yi, J. Lee, Toxic effects of titanium dioxide nanoparticles on microbial activity and metabolic flux, Biotechnol. Bioprocess Eng. 17 (2012) 276–282, https://doi.org/10.1007/s12257-010-0251-4.